Biomass Conversion and Biorefinery
https://doi.org/10.1007/s13399-024-05584-4

ORIGINAL ARTICLE

Influential lead uptake using dried and inactivated-fungal biomass obtained from *Panaeolus papilionaceus*: biological activity, equilibrium, and mechanism

Zeynep Mine Şenol[1] · Zehra Saba Keskin[2] · Emine Dinçer[1] · Amina Ben Ayed[3]

Received: 8 January 2024 / Revised: 13 March 2024 / Accepted: 30 March 2024

Abstract
In this study, the use of fungal (*Panaeolus papilionaceus*) biomass as a biosorbent was investigated to effectively remove Pb^{2+} ions from aquatic medium. The removal of Pb^{2+} ions using a fungal biosorbent was examined in a batch system in terms of initial solution pH, temperature, time, and initial Pb^{2+} concentration. Optimal operating conditions for biosorption of Pb^{2+} ions; pH: 4.5, T: 25 °C, and t: 24 h. The max biosorption capacity for Pb^{2+} ions was found to be 31.2 mg g^{-1} from the Langmuir model. Thermodynamic studies showed that Pb^{2+} ions biosorption into fungal biomass was possible, spontaneous, and endothermic. Additionally, the antimicrobial activity and antibiofilm activity of the extract of fungus were also investigated. It was determined that the fungal extract did not have antimicrobial properties. On the other hand, the extract has been shown to have the potential to prevent biofilm formation. 1 mg of the extract prevented the biofilm formation of *Staphylococcus aureus* by 87.85%. It has been observed that the biosorption mechanism of Pb^{2+} ions into fungal biomass includes the steps of surface biosorption, film diffusion, and intra-particle diffusion.

Keywords Adsorption · Fungal biosorbent · *Panaeolus papilionaceous* · Pb^{2+} · Wastewater treatment

1 Introduction

Today, the presence of heavy metals uncontrollably discharged into water bodies as a result of anthropogenic activities and rapid industrialization has become a global threat [1]. Heavy metals in dissolved or particle forms such as lead (Pb), mercury (Hg), copper (Cu), cadmium (Cd), zinc (Zn), and nickel (Ni) harm ecological systems because they are non-biodegradable and remain stable [2, 3]. Pb is one of the most common toxic heavy metals found in industrial wastewater, owing to its widespread use in various industrial processes such as mining, automotive manufacturing, battery production, and metal plating [4]. However, the World Health Organization (WHO) has reported that the maximum allowable concentration of Pb^{2+} ions in wastewater and drinking water should be 0.05 mg L^{-1} and 0.01 mg L^{-1}, respectively [5]. Exceeding these limits in water consumption can lead to various health issues in living beings, including kidney, brain, and liver damage, hypertension, anemia, as well as neurological and hematological disorders [6, 7]. Therefore, effectively removing Pb^{2+} ions pollution from water bodies is critical for human health [8, 9]. Adsorption is a low-cost, simple, and efficient method, offering higher selectivity than alternatives such as coagulation, membrane removal, ion exchange, and chemical precipitation [10]. However, adsorption efficiency may vary depending on factors such as the surface area of the adsorbent, pore volume and size, and functional groups present on the surface [11, 12].

Biomass (biosorbents) has attracted the attention of researchers as an environmentally friendly, biodegradable, and cost-effective option for removing low concentrations of Pb^{2+} ions from wastewater [13]. These adsorbents are sustainable and do not cause secondary pollution, making them a promising solution for this issue [14]. Biosorbents

✉ Zeynep Mine Şenol
msenol@cumhuriyet.edu.tr

1 Faculty of Health Sciences, Department of Nutrition and Diet, Sivas Cumhuriyet University, 58140 Sivas, Türkiye

2 Health Services Vocational School, Department of Pharmacy, Sivas Cumhuriyet University, 58140 Sivas, Türkiye

3 Laboratory of Multifunctional Materials and Applications (LaMMA), Faculty of Sciences of Sfax, University of Sfax, BP 1171, 3000 Sfax, Tunisia

Published online: 15 April 2024

such as bacteria [15], algae [16], fungi [17], plant residues [18], activated sludge [19], biopolymers [20], and yeast [21] have been investigated in Pb^{2+} ions removal studies.

Fungi are organisms with robust structures found worldwide, possessing physical properties that render them suitable for use as biosorbents [22]. They are increasingly employed in removal studies due to the diverse array of functional compounds present in their cell walls, as well as their low cost, ease of growth, simple fermentation techniques, and industrial abundance [23]. Fungal cell walls contain polysaccharides, lipids, and proteins with metal-binding functional groups, such as hydroxyl, carbonyl, carboxyl, amine, and amide [24]. These compounds enable fungi to efficiently remove heavy metals. Macrofungi such as *Phanerochaete chrysosporium* [25], *Lentinula edodes*, *Agaricus bisporus* [26], and *Ganoderma lucidum* [27] have been investigated for their ability to remove Pb^{2+} ions via biosorption. This study explores the potential of using inactivated and dried *P. papilionaceus* as a sustainable, inexpensive, readily available, and environmentally friendly biosorbent for removing Pb^{2+} ions from aqueous media. *P. papilionaceus* is a small, brown-blackish colored mushroom with conical or bell-shaped caps from the *Bolbitiaceae* family, inedible, non-poisonous, with remarkable health benefits and a common species [28].

In the literature review, no study was found investigating the biosorption capacity of P. papilionaceus. Therefore, the current study is significant as it represents the first exploration into this subject. The surface morphology and chemical structure of P. papilionaceus before and after biosorption were examined using FTIR, SEM, and EDX characterization techniques. Studies were conducted under various parameters including solution pH, contact time, amount of biosorbent, temperature, and initial Pb^{2+} ions concentration to assess their effects on the biosorption process. In addition, the determination of the antimicrobial and antibiofilm properties of *P. papilionaceus* was also investigated in the study.

2 Material and method

2.1 Chemicals and instrumentation

$Pb(NO)_3$, KNO_3, HCl, HNO_3, NaOH, ethyl alcohol, and all other chemicals were of analytical purity (Sigma Aldrich).

The functional groups on the fungal biosorbent before/after Pb^{2+} ions biosorption were determined using the FT-IR (ATR, Bruker Model: Tensor II) technique. The changes in surface morphology of the fungal biosorbent before/after Pb^{2+} ions biosorption, along with the identification of different elements, were analyzed by SEM–EDX (TESCAN MIRA3 XMU). The Pb^{2+} ion concentrations were determined using the PAR method [29] with a UV–vis spectrophotometer (UV-DR-6000; Shimadzu, China) at $\lambda = 519$ nm. Fatty acid methyl esters in the fungi sample were analyzed by gas chromatography using flame ionization detection (GC-FID) equipment (Shimadzu, QP2010) and DB FastFame capillary column [30].

2.2 Preparation of biosorbent

Fungal biosorbent was collected from Sivas, Turkey. The sample was photographed in the field and then transported to the laboratory by being carefully wrapped in individual paper parcels to prevent damage. The samples were diagnosed based on field data and microscopic features observed in laboratory examinations. Then, the biosorbent was washed several times with deionized water and then ıt was dried at 25 °C. It was then stored in a polystyrene container to be used in biosorption studies.

2.3 Biosorption procedure

Pb^{2+} ions biosorption was investigated using the batch biosorption method. The main factors examined are pH, contact time, adsorbent amount, temperature, and initial Pb^{2+} concentration. In each experimental set, a fixed dosage of 50 mg of biosorbent was added to 10 mL solutions consisting of 1000 mg L^{-1} Pb^{2+} with stirring for 24 h at room temperature. Then, the supernatant concentration and maximum absorbance of 519 nm for Pb^{2+} ions were measured. Pb^{2+} ion concentration was determined by the absorbance measurement. The batch adsorption conditions are given in Table 1. Q (mg g^{-1}) and Biosorption% were calculated using (1) and (2) [31];

$$Q = \left[\frac{C_i - C_f}{m}\right] xV \tag{1}$$

$$Biosorption\% = \left[\frac{C_i - C_f}{C_i}\right] x100 \tag{2}$$

2.4 Preparation of the fungi extract for biological activity

The fungi extract, intended for use in antibacterial and antibiofilm activity studies, was prepared using the Soxhlet extraction method. Fungi sample was dried and pulverized into a fine powder by grinding them in a mortar. The extraction process was conducted for 12 h in 400 mL methanol. Following the extraction, the methanol was removed at 40 °C using an evaporator, resulting in the isolation of a dry, pure substance.

Table 1 Batch biosorption experiment conditions

Experiment	Solution pH	Inital Pb^{2+} conc. (mg L^{-1})	Contact time (min)	Temperature (^{0}C)
Effect of pH	1.0–5.0	500	1440	25
Effect of concentration	4.5	50–1000	1440	25
Effect of contact time	4.5	500	2–1440	25
Effect of temperature	4.5	500	1440	5, 25, 40

For the preparation of the main stock extract solution, 0.15 g of extract was dissolved in 3 mL of methanol. After sterilization with a 0.22 µm diameter syringe filter, the main stock solution was immediately used for bioactivity analysis. The rest of the pure substance was stored at + 4 °C.

2.5 Assessment of antibacterial activity

The antibacterial activity of fungi extract was assessed using the micro-broth dilution method, following the guidelines developed by the Clinical and Laboratory Standards Institute (CLSI) (Clinical and Laboratory Standards Institute, 2019). The study used a total of 6 different indicator bacteria, comprising 3 g-positive and 3 g-negative species. Indicator microorganisms include *Listeria monocytogenes* ATCC 7644, *Bacillus subtilis* (ATCC 6633) and *Staphylococcus aureus* (ATCC 43300), *Escherichia coli* (ATCC 25922), *Klebsiella pneumoniae* (ATCC 10031) and *Pseudomonas aeruginosa* (ATCC 27853). Ciprofloxacin was used as a control drugs. The sample and inoculum were prepared as follows.

For inoculum preparation, the indicator bacteria were cultured in Mueller Hinton Broth (MHB) at 37 °C for an overnight period. Subsequently, the density was adjusted to McFarland no 0.5 standard, and an additional dilution of 100 fold was performed in MHB to obtain an inoculum at a concentration of 10^6 colony-forming units per milliliter (CFU/mL). For sample preparation, the fungi extract was diluted in MHB within a concentration range of 2 mg/mL to 0.0312 mg/mL.

To analyze, 100 µl of the prepared dilutions of fungi sample and 100 µl inoculum were transferred to sterile ELISA plates. The plates were incubated at 37 °C for 24 h. Following the incubation period, the absorbance values of the plates were read at 600 nm by BMG LABTECH's ultra-fast UV/vis spectrophotometer (SPECTROstar Nano, Germany). Thus, in the final analysis, antibacterial activity was evaluated in the concentration range of 1 mg to 0.0156 mg. The analysis was repeated twice. The well in which the minimum inhibitory concentration (MIC) was seen was identified, and the corresponding MIC value was computed.

To ascertain the absence of any impact of the solvent itself on bacterial growth, a control experiment was conducted. This control involved the use of inoculated broth supplemented solely with methanol, at the same dilutions employed in the experimental procedures.

2.6 Assessment of antibiofilm activity

The assessment of antibiofilm activity was conducted using a modified version of the Christensen method, as originally suggested by Christensen et al. [32]. In parallel with the antibacterial activity study, a total of 6 bacteria species (identical to the aforementioned in the antibacterial activity study) were used as indicator bacteria.

For inoculum preparation, the indicator bacteria were cultured in Tryptic Soy Broth (TSB) supplemented with 2% glucose at 37 °C for an overnight period and, the density was adjusted to McFarland no 0.5 standard to obtain an inoculum at a concentration of 10^8 CFU/mL. For sample preparation, the fungi extract was diluted in TSB supplemented with 2% glucose within a concentration range of 2 mg/mL to 0.0312 mg/mL.

To biofilm formation, 100 µl of the prepared dilutions of fungi sample and 100 µl inoculum were transferred to sterile ELISA plates. Then, the plates were incubated at 37 °C for 48 h. Thus, in the final analysis, antibiofilm activity was evaluated in the concentration range of 1 mg to 0.0156 mg. To assess the biofilm inhibition, after the incubation period, the medium present in the wells was discarded and, the plates were washed by using phosphate buffered saline solution. Following the washing step, plates were kept at 25 °C for 2 h. Then 1% crystal violet solution (200 µl) was added the each well, after waiting 15 min, and then washed by using phosphate-buffered saline solution. Finally, 200 µL absolute ethanol was added to the wells to dissolve the crystal violet and the absorbance values of the plates were read at 600 nm by BMG LABTECH's ultra-fast UV/vis spectrophotometer (SPECTROstar Nano, Germany). Results were calculated as % biofilm inhibition concentration. In the analyses, Indicator bacterial suspensions (200 µl) were used as negative control and TSB containing 2% glucose was used as positive control.

3 Results and discussion

3.1 Effect of pH on adsorption and pHpzc for fungal biosorbent

One of the vital parameters affecting biosorption efficiency in the biosorption process is the initial pH value of the medium. The solution for fungal biosorbent Pb^{2+} ion

biosorption was investigated in the pH range of 1.0–5.0 and the results obtained are shown in Fig. 1. When Fig. 1 is examined, it was seen that there was an increase in biosorption efficiency from 26 to 56% as the pH value increased from pH:1.0 to pH:4.0. After pH: 4.0, biosorption efficiency decreased relatively.

At low pH values, biosorption efficiency decreases due to partial protonation of surface functional groups of the fungal biosorbent and strong competition between H^+ ions and Pb^{2+} ions. Since there is competition between H^+ ions and Pb^{2+} ions for binding sites at low pH values, biosorption efficiency is less at low pH values. With increasing pH values, the surface functional groups became deprotonated, causing strong electrostatic interactions with Pb^{2+} ions, and biosorption increased. It was observed that Pb^{2+} ion biosorption reached its maximum at pH: 4.0. After pH: 4.0, biosorption was observed to decrease relatively.

At high pH values, metal hydroxides of Pb^{2+} ions begin to precipitate. At pH > 5.5, Pb^{2+} ions undergo a series of hydrolysis reactions and as a result, hydroxide species are formed [33]. In this case, the repulsion forces between the functional groups on the adsorbent surface and the Pb^{2+} ions in the solution decrease, and the number of Pb^{2+} ions removed from the solution decreases. For this reason, Pb^{2+} ions were not studied since they tend to precipitate at pH > 5.5.

The zero charge point (pHpzc) represents the pH value at which the biosorbent surface is electrically neutral. The surface charge solid addition technique of fungal biosorbent was found by adding the same amount of solid to a series of solutions with the same ionic strength at different pH values [34]. The pHpzc value for the fungal biosorbent was found to be 4.49 (Fig. 2).

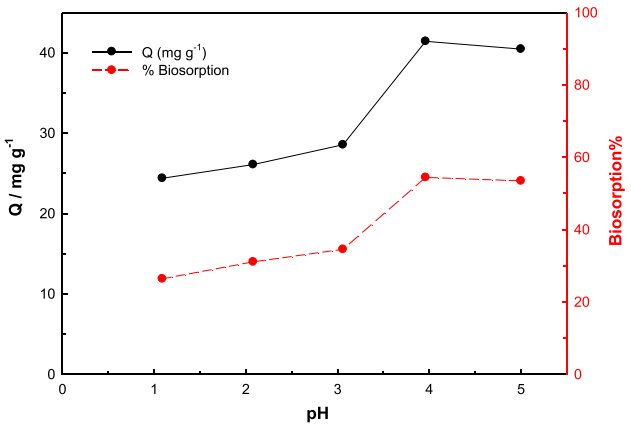

Fig. 1 Effect of pH on biosorption {$[Pb^{2+}]_0$: 500 mg L^{-1}, biosorbent dosage:10 g L^{-1}, pH:1.0–5.0, contact time:24 h, temperature: 25 °C}

3.2 Effect of biosorbent dose

The effect of fungal biomass amount on Pb^{2+} ion biosorption was (Fig. 3). Figure 3 shows that the adsorption rate increases from 28 to 85% with the increase of the fungal dosage from 1 to 20 g L^{-1}, while the quantity adsorbed decreases from 75 to 40 mg g^{-1}. The amount of Pb^{2+} removed increases with the biosorbent mass because more active sites can be accessed to take part in the biosorption process [35]. Fungal cell walls contain various functional groups such as carboxyl, hydroxyl, amino, sulfhydryl, and phosphate [36]. These functional groups are also of interest for Pb^{2+} ions. This reveals the excellent biosorption properties of fungi.

3.3 Biosorption isotherms

Biosorption equilibrium isotherms, whether graphical or mathematical, play a crucial role in understanding and

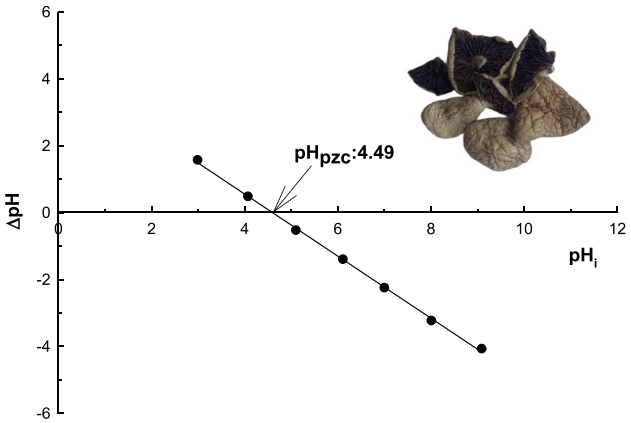

Fig. 2 pHpzc for fungal biosorbent

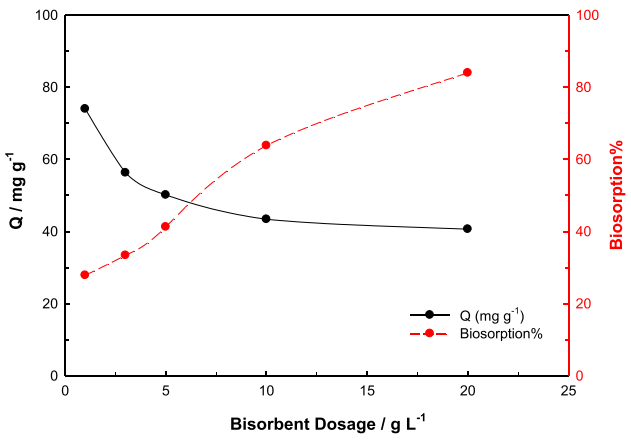

Fig. 3 Effect of biosorbent dose on biosorption {$[Pb^{2+}]_0$: 500 mg L^{-1}, biosorbent dosage: 1, 3, 5, 10 and 20 g L^{-1}, natural pH:4.5, contact time:24 h, temperature: 25^0C}

describing biosorption processes. They provide valuable information about how a biosorption system reaches equilibrium and the characteristics of the biosorbent involved in the process. These isotherms are used to elucidate the fundamental nature of biosorption, the mechanisms behind it, the optimum biosorption capacity, and the affinity of the biosorbent for the target substances in a solution [37].

Langmuir [38], Freundlich [39], and D-R [40] isotherm models were used to explain the concentration effect on biosorption. Nonlinear biosorption isotherms for Pb^{2+} ions into the fungal biosorbent are presented in Fig. 4, and the equations and determine parameters of these isotherms are presented in Table 2. The optimum biosorption capacity (Q_L) determined for the fungal biosorbent from the Langmuir biosorption isotherm model was calculated as 31.2 mg g^{-1}. The K_L was determined as 0.745 L mg^{-1}. When the Freundlich and Langmuir isotherm models are compared, it is understood that the R^2 value of the Freundlich model is higher and it is the model that describes the biosorption process better. This shows that biosorption follows multilayer biosorption behavior [41]. Freundlich capacity (X_F) was determined as 3.89 and heterogeneity factor (β) was determined as 0.332. Since the E_{DR} value was found as 11.9 kJ mol^{-1}, it was concluded that the biosorption process proceeded chemically. The maximum biosorption capacity of the fungal biosorbent determined for the removal of Pb^{2+} ions and the isotherm model they are compatible with are compared with various sorbents in Table 3. As a result of this comparison, it was determined that the maximum biosorption capacity of fungal biomass was high enough to be an alternative to other sorbents. This indicates that the fungal biosorbent is a competitive and potentially cost-effective alternative to other sorbents for the removal of Pb^{2+} ions from solutions.

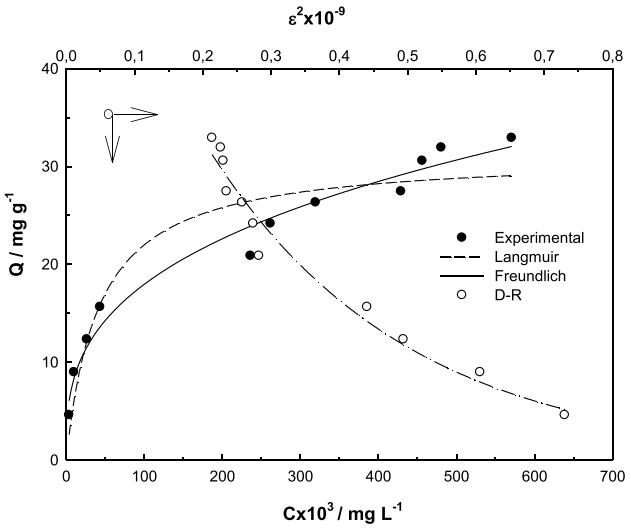

Fig. 4 Biosorption isotherms {$[Pb^{2+}]_0$: 50–1000 mg L^{-1}, biosorbent dosage:10 g L^{-1}, natural pH:4.5, contact time:24 h, temperature: 25 °C}

Table 2 Parameters calculated from isotherm models

Isotherm Model	Parameter	Value
Langmuir $Q = \frac{Q_L C_e}{1+K_L C_e}$	Q_L (mg g^{-1})	31.2
	K_L (L mg^{-1})	0.745
	R^2	0.912
Freundlich $Q = X_F C_e^{\beta}$	X_F	3.89
	β	0.332
	R^2	0.975
D-R $Q = X_{DR} e^{-(K_{DR}\varepsilon^2)}$ $\varepsilon = RT\ln\left(1+\frac{1}{C_e}\right)$ $E_{DR} = (2K_{DR})^{-0.5}$	X_{DR} (mg g^{-1})	65.7
	$-K_{DR}x10^9$/mol^2 KJ^{-2}	3.48
	E_{DR}/kJ mol^{-1}	11.9
	R^2	0.968

3.4 Biosorption kinetics

The mechanism of the biosorption process depends on the chemical and physical properties of the biosorbent as well as the system conditions. The biosorption process must reach equilibrium in a short time. Because increasing contact time may cause higher treatment costs in wastewater treatment plants. When Fig. 5 was examined, it was observed that Pb^{2+} ion biosorption increased with contact time. It was observed that biosorption was rapid until the first 240 min and reached equilibrium after that. The high biosorption rate in the first 240 min is initially due to the number of empty active centers present in the fungal biosorbent. Therefore, increasing concentration gradients exist between Pb^{2+} ions in solution and the surface of the fungal biomass. This increase in the concentration gradient causes an increase in the removal rate of Pb^{2+} ions in the initial stages. Over time, this concentration decreases due to Pb^{2+} ions adhering to empty active centers, which causes the adsorption rate to decrease.

Experimental data were applied to pseudo first order (PFO) [48], pseudo second order (PSO) [49], and intra particle diffusion (IPD) [50] models to predict the mechanism involved in the biosorption process [51, 52]. The applicability of PFO and PSO kinetic models in the removal of Pb^{2+} ions using fungal biomass was evaluated by comparing their correlation coefficients and the most appropriate model was selected. According to Table 4, it can be seen that the R^2: 0.777 value of the PFO model is smaller than the R^2: 0.834 value of the PSO model. In addition, it has been determined that the theoretical Q_t value and the experimental Q_e values of the PSO model are in agreement with each other in explaining the experimental data. It was seen that the PSO model described the biosorption process better. The multicollinearity of the Q-$t^{0.5}$ graph drawn using experimental data indicates that the

Table 3 Isotherm modeling on the biosorption of Pb^{2+} ions onto another sorbent in literature

Adsorbent	pH	Q/ mg g^{-1} from Langmuir model	Best-fitted isotherm model	Reference
Oxidized maple wood biochars	4.0	10.8	Langmuir	[42]
Lantana camara leaves	6.0	3.51	Langmuir	[6]
Rosa damascena waste	6.5	24.9	Langmuir	[4]
Chitosan-polyvinyl alcohol	3 – 4	4.02	Langmuir	[43]
Bi-functional β-cyclodextrin polymer	-	113	Langmuir	[44]
Shanghai silty clay	6	26.5	Langmuir	[45]
Xanthan biopolymer integrated graphene oxide	5.2	199	Langmuir	[46]
Chitosan-bentonite composite beads	4.5	88.1	Langmuir	[47]
Rhizopus arrhizus	4.0	104	Langmuir	[17]
Panaeolus papilionaceus	4.5	31.2	Freundlich	This study

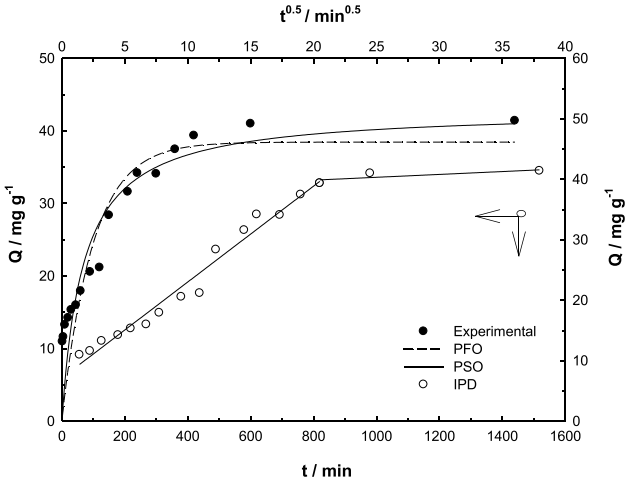

Fig. 5 Biosorption kinetics {$[Pb^{2+}]_0$: 500 mg L^{-1}, biosorbent dosage:10 g L^{-1}, natural pH:4.5, contact time:2–1440 min, temperature: 25 °C}

Table 4 The calculated parameters from kinetic models

Kinetic model	Parameter	Value
PFO	Q_t/mg g^{-1}	41.4
$Q_t = Q_e\left[1 - e^{-k_1 t}\right]$	Q_e/mg g^{-1}	38.5
$H_1 = k_1 Q_e$	$k_1 \times 10^3$/min^{-1}	10.1
	$H_1 \times 10^3$/mg g^{-1} min^{-1}	389
	R^2	0.777
PSO	Q_t/mg g^{-1}	41.4
$Q_t = \frac{t}{\left[\frac{1}{k_2 Q_e^2}\right] + \left[\frac{t}{Q_e}\right]}$	Q_e/mg g^{-1}	42.9
	$k_2 \times 10^3$/mg^{-1} g min^{-1}	0.344
$H_2 = k_2 Q_e^2$	$H_2 \times 10^3$/mg g^{-1} min^{-1}	633
	R^2	0.834
IPD	$k_i \times 10^3$/mg g^{-1} $min^{-0.5}$	7140
$Q_t = k_i t^{0.5}$	R^2	0.975

biosorption mechanism follows two or more steps (Fig. 6). When Fig. 6 is examined, it is seen that the IPD model graph is divided into two linear parts. The first linear part of the IPD model plot shows a boundary layer effect, while the second linear part represents intra-particle diffusion. When all this information was evaluated together, it was concluded that the biosorption process followed the PFO and IPD models.

3.5 Biosorption thermodynamics

To explain the thermodynamic behavior of the biosorption process, the studies were carried out at 5 °C, 25 °C, and 40 °C. Thermodynamic parameters were derived from data obtained from temperature effect studies on biosorption (Eq. 3–6). The following equations were used to determine the ΔH^o, the ΔS^o, and the ΔG^o parameters [53].

$$K_d = \frac{Q}{C_e} \tag{3}$$

$$\Delta G^{\circ} = -RTln\left(K_d\right) \tag{4}$$

$$lnK_D = \frac{\Delta S^{\circ}}{R} - \frac{\Delta H^{\circ}}{RT} \tag{5}$$

$$\Delta G^o = \Delta H^o - T\Delta S^o \tag{6}$$

As seen in Fig. 6, a 1/T graph was drawn against ln K_d for Pb^{2+} removal on the fungal biosorbent. Figure 6 represents a graph where 1/T is plotted against ln K_d (the natural logarithm of the distribution coefficient) for the removal of Pb^{2+} ions on the fungi. ΔS^o was calculated from the intersection point of this obtained graph, and ΔH^o was determined from the slope of the ln K_d vs. 1/T graph. The obtained parameters

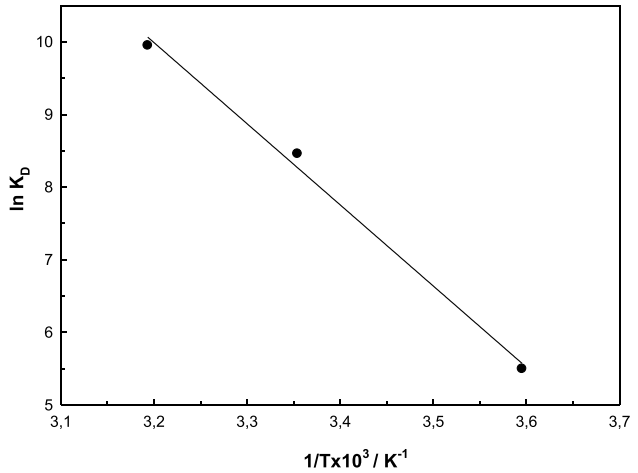

Fig. 6 Biosorption thermodynamics {$[Pb^{2+}]_0$: 500 mg L^{-1}, biosorbent dosage:10 g $L.^{-1}$, natural pH:4.5, contact time:24 h, temperature: 5 °C, 25 °C, ve 40 °C}

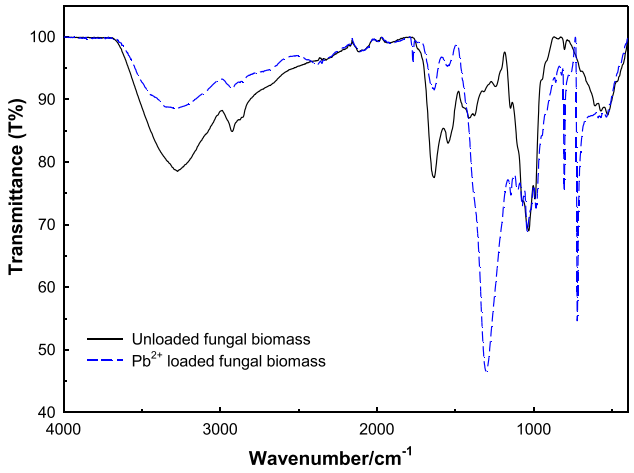

Fig. 7 FT-IR spectra of fungal biomass (**a**) Pb^{2+} biosorbed fungal biomass (**b**)

are given in Table 5. The positive ΔH^o value of 92.9 kJ mol^{-1} determined for Pb^{2+} biosorption indeed indicates an endothermic nature of the biosorption process. The positive ΔS^o value of 380 kJ mol^{-1} determined for the biosorption process indicates that randomness increases at the biosorbate-biosorbent interface during the process and ion exchange reactions occur [54]. Additionally, high negative ΔG^o values indicate that biosorption occurs chemically [55].

3.6 FT-IR and SEM–EDX analyses

FT-IR analysis was performed to identify surface functional groups of the fungus as well as groups that would assist in Pb^{2+} biosorption. FT-IR spectra of the fungus before and after Pb^{2+} biosorption are given in Fig. 7 (a, b). The broad and strong band in the range of approximately 3000–3600 cm^{-1} observed in the FT-IR spectrum of fungus without Pb^{2+} loading can be explained by the stretching vibration of –OH and N–H groups [56]. The observed peak at 2926 cm^{-1} can be attributed to the symmetric and asymmetric vibration of the CH_3 and CH_2 groups [57], and the peak at 1638 cm^{-1} can be attributed to the stretching vibration of the carboxyl group (-COOH) [22]. In addition, the peaks at 1539 cm^{-1}, 1410 cm^{-1} and 1040 cm^{-1} can be associated with the amide (II) vibration, bending vibration of the C-H group, and stretching vibrations of the C-O-C and C-O groups, respectively. The peak observed at 609 cm^{-1} can be explained as the vibration of phosphate groups (P = O) [58]. In line with this information obtained from the FTIR spectrum, it was determined that the fungus has functional groups that help metal biosorption such as carboxyl, hydroxyl, amino, and amide. When looking at the FT-IR spectrum of the fungus after Pb^{2+} biosorption, a shift in some characteristic absorption peaks and an increase or decrease in their intensity were detected. It is observed that the peaks where the vibrations of –CH, -COOH, C-O, and phosphate groups detected in the structure of the fungus are determined to have shifted to 2916 cm^{-1}, 1623 cm^{-1}, 1310 cm^{-1}, 732 cm^{-1}, respectively. The changes observed before and after biosorption can be attributed to surface complexation and electrostatic interaction reactions between these functional groups and Pb^{2+} ions [58].

Table 5 Thermodynamic parameters

Temperature/°C	ΔH^0/kJ mol^{-1}	ΔG^0/kJ mol^{-1}	ΔS^0/ $Jmol^{-1}$ K^{-1}	R^2
5	92.9	-12.8	380	0.995
25		-20.5		
40		-26.1		

SEM images of the fungal biosorbent before and after Pb^{2+} ion biosorption are given in Fig. 8. In the SEM image of the fungal biomass, the structure consisting of sporangiospore mass is seen (Fig. 8 (a)). The SEM image of the fungal biomass (Fig. 8 (a)) was observed to be obviously different from that of the Pb^{2+} ions biosorbed (Fig. 8 (b)). It was seen that the sporangium surface of the fungus became irregular and rough after the biosorption of Pb^{2+} ions. As shown in Fig. 8 (c-d), EDX analysis results showed that there were changes in percentage by weight in the inorganic components after Pb^{2+} ions biosorption, and there were increases and decreases indicating ion exchange. Based on this information, it was thought that more than one mechanism was involved in Pb^{2+} ion biosorption onto fungal biomass, such as surface complexation and electrostatic interactions.

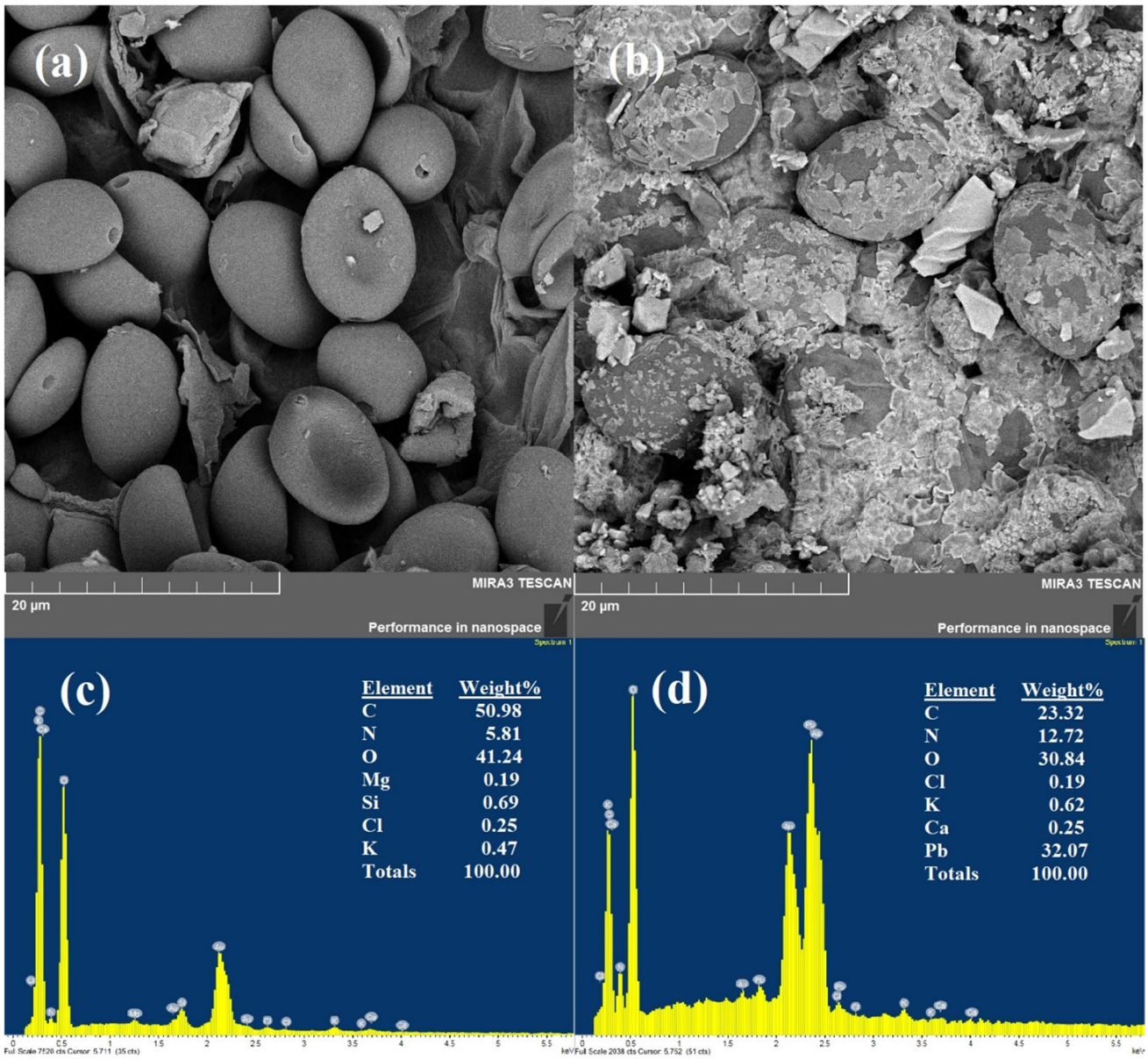

Fig. 8 SEM images of fungal biomass (**a**) Pb^{2+} biosorbed fungal biomass (**b**)

3.7 Biological activity of the fungal extract

Certain species belonging to the Panaeolus genus have garnered attention due to their notable psilocin production, as well as their diverse range of biological activities, including antioxidative, anti-inflammatory, and antibacterial capabilities. However, there is limited data available regarding the antibacterial properties of *P. papilionaceus*, a species known for its capability to produce psychoactive compounds. Although Coprophilous mushroom species are generally considered to have a high potential for producing antimicrobial compounds, the limited number of studies conducted on this subject indicate the absence of antimicrobial activity by this species [59]. The current investigation aimed to evaluate the antibacterial efficacy of the methanol extract derived from *P. papilionaceus* against a selected set of six distinct bacterial strains. However, it was shown that there was no notable impact on any of the bacteria examined when exposed to concentrations ranging from 1 to 0.0156 mg.

In the current study, were examined not only the antimicrobial effects of the fungal extract but also its ability to inhibit biofilm formation. Biofilms are complex structures that result from the attachment of microbes to one other and a surface, accompanied by the release of extracellular polymeric substrates (EPS) into the surrounding environment.

Microorganisms engage in the formation of biofilms as a means to enhance their resilience against antimicrobial substances and various environmental stressors present in natural settings. The production of biofilms is considered unfavorable in terms of hygiene and safety, especially within the food industry, due to its propensity to facilitate the attachment of pathogenic microbes or those responsible for food spoiling onto food and related surfaces. Therefore, understanding the formation of biofilms on surfaces and their removal is of great importance [60]. There is a lack of available evidence related to the antibiofilm capabilities exhibited by *Panaeolus* species, including *P. papilionaceus*. To the best of our current understanding, this study represents the initial documentation of the anti-biofilm properties of *P. papilionaceus*. The findings of our investigation revealed that *P. papilionaceus* could prevent biofilm formation at varying rates depending on the type of biofilm-forming bacteria (Table 6). It was determined that 1 mg of fungal extract noteworthy inhibitory effect on the formation of biofilms by indicator bacteria, particularly *S. aureus* and *Klebsiella*, with reductions of 87.85% and 72.73% respectively. However, no discernible impact was observed on the biofilm formation of *P. aeruginosa* and *B. subtilis*. Upon analysis of the fungal sample, it was determined that the predominant fatty acid component was linoleic acid (%80.6) (Fig. 9). In addition to linoleic acid, the presence of palmitic acid, stearic acid, and oleic acid in small amounts has also been observed.

Table 6 Reduction in biofilm formation on 1 mg mL^{-1} concentration

Indicator Bacteria	Biofilm inhibition ratio %
Listeria monocytogenes ATCC 7644	62.68 ± 0.93
Bacillus subtilis (ATCC 6633)	ND
Klebsiella pneumoniae (ATCC 10031)	87.85 ± 0.47
Pseudomonas aeruginosa (ATCC 27853)	ND
Staphylococcus aureus (ATCC 43300)	72.73 ± 1.95
Escherichia coli (ATCC 25922)	56.35 ± 3.21

ND: no antibiofilm activity

3.8 Biosorption mechanism

The biggest challenge in a biosorption study is to elucidate the biosorption mechanism. To elucidate the biosorption mechanism, the surface properties and structure of the biosorbent need to be examined. In this context, it should be noted that; Fungi are biological materials that can remove pollutants such as heavy metals and dyes [2]. The binding mechanism of heavy metals to fungi can be explained by the strong attraction forces of cell wall components. Fungi have great advantages over other biosorbent materials in terms of biosorption and bioaccumulation activities due to their cell wall materials showing metal binding properties [61]. The fungal cell wall consists of glycoproteins, chitin, and glucans, as well as chitosan and other components [62]. The complex structure of fungal cell walls containing various functional groups such as hydroxyl (OH^-), carboxyl ($COOH^-$), amino (NH_2), phosphate (PO_4^{3-}), and sulfhydryl (SH^-) reveals the excellent biosorption properties of fungi (confirmed by the FT-IR spectrum, SEM images, and fatty acid profile). The biosorption mechanism is assumed to include the following steps [63]; i) bulk solution transport to the surface of the biosorbent, ii) diffusion of Pb^{2+} ions across the boundary layer to the surface of the fungal biosorbent (film

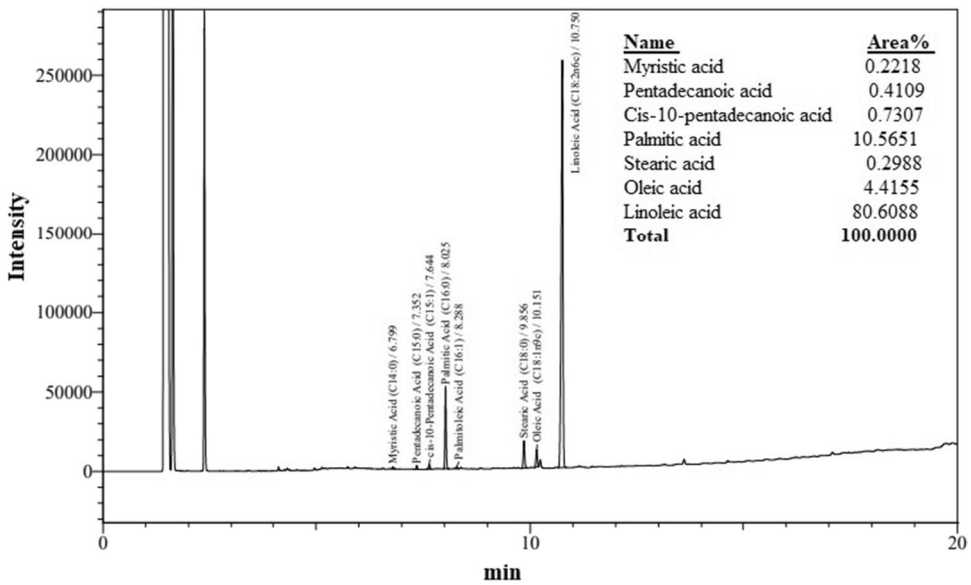

Fig. 9 Fatty acid profile of fungal (*Panaeolus papilionaceus)* biosorbent

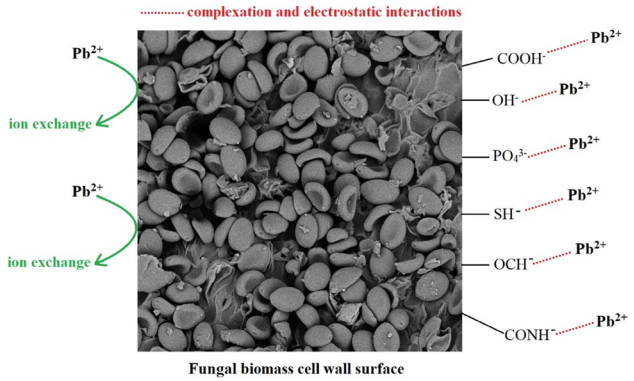

Fig. 10 Biosorption mechanism of fungal biomass

diffusion), iii) accumulation of increasing amount of Pb^{2+} ions to the surface of the fungal biosorbent (biosorption). Electrostatic interactions occur between biological groups such as OH^-, $COOH^-$, NH_2, PO_4^{3-}, SH^-, and Pb^{2+} ions in the fungal biosorbent cell wall, which is one of the active centers for biosorption. Additionally, during the process of biosorption to the fungal surface, chelation occurs between one or more Pb^{2+} ions in the solution and the active functional groups on the fungal cell wall surface. In addition, solution pH supports ion exchange because at the natural pH of Pb^{2+} ions: 4.5, the competitive effect of H^+ ions decreases, and negative ion gaps are formed on the fungal cell wall surface that can biosorb more Pb^{2+} ions. iv) Pb^{2+} ions into the internal pores and capillary spaces of the fungal biosorbent (intra-particle diffusion). Each of these four mechanisms are independent process (Fig. 10). When all this information is evaluated together, it is thought that the biosorption process of Pb^{2+} ions into fungal biomass is accompanied by the steps of surface biosorption, intra-particle diffusion, and film diffusion on the fungal cell walls. In addition, during the biosorption process, protons or light metal cations such as Na^+, K^+, Mg^{2+}, and Ca^{2+} attached to the functional groups on the biosorbent surface are exchanged with metal cations in the aqueous solution (ion exchange) [64].

4 Conclusion

In this study, to effectively remove Pb^{2+} ions from aqueous solutions fungal (*P. papilionaceus*) biomass was used. The optimum biosorption of Pb^{2+} ions was achieved in 240 min at 25 °C at a natural pH of 4.5. It was observed that biosorption isotherms fit the Freundlich model better. The optimum biosorption capacity calculated from the Langmuir model was found to be 31.2 mg g^{-1}. The biosorption energy found from the D-R model showed that the biosorption process was chemical. Negative values of the Gibbs free energy change, one of the thermodynamic parameters, showed that the biosorption process was spontaneous, and positive enthalpy values showed that the biosorption process was endothermic. Biosorption kinetics showed that the biosorption process followed PSO and IPD patterns. Biosorption of Pb^{2+} ions into fungal biomass was observed to involve surface biosorption, film diffusion, and intra-particle diffusion mechanisms. In light of all this information, it was seen that the fungal biosorbent is a low-cost, natural, effective, and potentially promising biosorbent in the removal of Pb^{2+} ions from aqueous solution.

Author contribution Zeynep Mine Şenol: experimental work, visualization, methodology, supervision, writing, guidance, editing, and review. Zehra Saba Keskin: experimental work, visualization, methodology writing, editing, and review. Emine Dinçer: experimental work, biological analysis, writing, editing, and review. Amina Ben Ayed: writing, editing, and review.

Funding Open access funding provided by the Scientific and Technological Research Council of Türkiye (TÜBİTAK). The present study was partly supported by the Sivas Cumhuriyet University Projects Commission.

Data availability Not applicable.

Declarations

Ethical approval Not applicable.

Competing interests The authors declare that they have no competing interests.

References

1. Alamrani NA, Almutairi FM, Alotaibi FA, Alenazi DAK, Monier M, Abdel-Latif DA, Elsayed NH (2023) Developing thiosemicarbazide-modified/ion-imprinted chitosan for selective cadmium ion biosorption. Mater Today Chem 30. https://doi.org/10.1016/j.mtchem.2023.101547
2. Vieira RHSF, Volesky B (2000) Biosorption: a solution to pollution? Int Microbiol 3:17–24

3. Samimi M, Nouri J (2023) Optimized zinc uptake from the aquatic environment using biomass derived from Lantana camara L. stem. Pollution. https://doi.org/10.22059/POLL.2023.363363.2014
4. Batool F, Mohyuddin A, Amjad A, ul Hassan A, Nadeem S, Javed M, Hafiz Dzarfan Othman M, Wayne Chew K, Rauf A, Kurniawan TA (2023) Removal of Cd(II) and Pb(II) from synthetic wastewater using Rosa damascena waste as a biosorbent: an insight into adsorption mechanisms, kinetics, and thermodynamic studies. Chem Eng Sci 280. https://doi.org/10.1016/j.ces.2023.119072
5. Wu S, Jiang H, Lu J (2023) Adsorptive performance and mechanism exploration of L-lysine functionalized celluloses for enhanced removal of Pb(II) from aqueous medium. Int J Biol Macromol 242. https://doi.org/10.1016/j.ijbiomac.2023.124997
6. Negi A, Joshi SK, Bhandari NS (2023) Estimation of sorption–desorption characteristics of biosorbent of Lantana camara leaves for removal of Pb (II) ions from wastewater. Environ Monit Assess 195. https://doi.org/10.1007/s10661-022-10629-0
7. Kumar K, Singh D (2023) Toxicity and bioremediation of the lead: a critical review. Int J Environ Health Res. https://doi.org/10.1080/09603123.2023.2165047
8. Samimi M, Shahriari-Moghadam M (2021) Isolation and identification of Delftia lacustris Strain-MS3 as a novel and efficient adsorbent for lead biosorption: Kinetics and thermodynamic studies, optimization of operating variables. Biochem Eng J 173. https://doi.org/10.1016/j.bej.2021.108091
9. Aljohani MS, Alnoman RB, Alharbi HY, Al-Anazia M, Monier M (2024) Designing of a cellulose-based ion-imprinted biosorbent for selective removal of lead (II) from aqueous solutions. Int J Biol Macromol 259:129145. https://doi.org/10.1016/j.ijbiomac.2023.129145
10. Mosoarca G, Vancea C, Popa S, Dan M, Boran S (2022) The use of bilberry leaves (Vaccinium myrtillus L.) as an efficient adsorbent for cationic dye removal from aqueous solutions. Polymers (Basel) 14. https://doi.org/10.3390/polym14050978
11. Rehman MU, Taj MB, Carabineiro SAC (2023) Biogenic adsorbents for removal of drugs and dyes: a comprehensive review on properties, modification, and applications. Chemosphere 338. https://doi.org/10.1016/j.chemosphere.2023.139477
12. Samimi M, Zakeri M, Alobaid F, Aghel B (2023) A brief review of recent results in arsenic adsorption process from aquatic environments by metal-organic frameworks: classification based on kinetics, isotherms and thermodynamics behaviors. Nanomaterials 13. https://doi.org/10.3390/nano13010060
13. Eliescu A, Georgescu AA, Nicolescu CM, Bumbac M, Cioateră N, Mureșeanu M, Buruleanu LC (2020) Biosorption of Pb(II) from aqueous solution using mushroom (Pleurotus ostreatus) biomass and spent mushroom substrate. Anal Lett 53. https://doi.org/10.1080/00032719.2020.1740722
14. Samimi M (2024) Efficient biosorption of cadmium by Eucalyptus globulus fruit biomass using process parameters optimization. Glob J Environ Sci Manag 10:27–38. https://doi.org/10.22034/gjesm.2024.01.03
15. Liu G, Geng W, Wu Y, Zhang Y, Chen H, Li M, Cao Y (2024) Biosorption of lead ion by lactic acid bacteria and the application in wastewater. Arch Microbiol 206:18. https://doi.org/10.1007/s00203-023-03755-x
16. Gu S, Lan CQ (2023) Effects of culture pH on cell surface properties and biosorption of Pb(II), Cd(II), Zn(II) of green alga Neochloris oleoabundans. Chem Eng J 468. https://doi.org/10.1016/j.cej.2023.143579
17. Senol ZM, Gül ÜD, Gurbanov R, Simsek S (2021) Optimization the removal of lead ions by fungi: Explanation of the mycosorption mechanism. J Environ Chem Eng 9. https://doi.org/10.1016/j.jece.2020.104760
18. Al-Amrani WA, Fathi NSSM, Hanafiah MAKM, Zakaria H (2023) Comparative biosorption of Cu (II) and Pb (II) Ions from aqueous solutions using soursop (Annona muricata L) leaf powder: characterisation, isotherm and kinetic studies. Bioresour Environ 1(1):66–79
19. Hua Liu G, Tang X, Yuan J, Li Q, Qi L, Wang H, Ye Z, Zhao Q (2023) Activated sludge process enabling highly efficient removal of heavy metal in wastewater. Environ Sci Pollut Res 30. https://doi.org/10.1007/s11356-022-23693-3
20. Berdous D, Abdellaoui N, Arous O, Akretche DE (2023) Low cost biopolymer adsorbents for the removal of heavy metal contaminant from wastewater. Macromol Symp 408. https://doi.org/10.1002/masy.202200066
21. Sagar Jena P, Pradhan A, Prakash Nanda S, Kishore Dash A, Naik B (2022) Biosorption of heavy metals from wastewater using Saccharomyces cerevisiae as a biosorbent: a mini review. Mater Today Proc 67. https://doi.org/10.1016/j.matpr.2022.07.306
22. Naeemullah, Tuzen M, Sarı A, Turkekul I (2020) Influential bioremoval of mercury using Lactarius acerrimus macrofungus as novel low-cost biosorbent from aqueous solution: Isotherm modeling, kinetic and thermodynamic investigations. Mater Chem Phys 249. https://doi.org/10.1016/j.matchemphys.2020.123168
23. Sharma R, Talukdar D, Bhardwaj S, Jaglan S, Kumar R, Kumar R, Akhtar MS, Beniwal V, Umar A (2020) Bioremediation potential of novel fungal species isolated from wastewater for the removal of lead from liquid medium. Environ Technol Innov 18:100757. https://doi.org/10.1016/j.eti.2020.100757
24. Ayele A, Haile S, Alemu D, Kamaraj M (2021) Comparative utilization of dead and live fungal biomass for the removal of heavy metal: a concise review. Sci World J 2021. https://doi.org/10.1155/2021/5588111
25. Huang C, Lai C, Xu P, Zeng G, Huang D, Zhang J, Zhang C, Cheng M, Wan J, Wang R (2017) Lead-induced oxidative stress and antioxidant response provide insight into the tolerance of Phanerochaete chrysosporium to lead exposure. Chemosphere 187. https://doi.org/10.1016/j.chemosphere.2017.08.104
26. Castanho NRCM, De Oliveira RA, Batista BL, Freire BM, Lange C, Lopes AM, Jozala AF, Grotto D (2021) Comparative study on lead and copper biosorption using three bioproducts from edible mushrooms residues. J Fungi 7. https://doi.org/10.3390/jof7060441
27. Rozman U, Kalčíková G, Marolt G, Skalar T, Žgajnar Gotvajn A (2020) Potential of waste fungal biomass for lead and cadmium removal: characterization, biosorption kinetic and isotherm studies. Environ Technol Innov 18. https://doi.org/10.1016/j.eti.2020.100742
28. Strauss D, Ghosh S, Murray Z, Gryzenhout M (2023) Global species diversity and distribution of the psychedelic fungal genus Panaeolus. Heliyon 9 https://doi.org/10.1016/j.heliyon.2023.e16338
29. Şenol ZM (2021) A chitosan-based composite for adsorption of uranyl ions; mechanism, isothems, kinetics and thermodynamics. Int J Biol Macromol 183:1640–1648. https://doi.org/10.1016/j.ijbiomac.2021.05.130
30. Zou Y, Yu H (2018) Improving the analysis of 37 fatty acid methyl esters using three types of capillary GC columns. Agilent Technologies Application Note
31. Samimi M, Mansouri E (2023) Efficiency evaluation of Falcaria vulgaris biomass in Co(II) uptake from aquatic environments: characteristics, kinetics and optimization of operational variables. Int J Phytoremediation. https://doi.org/10.1080/15226514.2023.2250462
32. Christensen GD, Simpson WA, Younger JJ, Baddour LM, Barrett FF, Melton DM, Beachey EH (1985) Adherence of coagulase-negative staphylococci to plastic tissue culture plates: a quantitative model for the adherence of staphylococci to medical devices. J Clin Microbiol 22. https://doi.org/10.1128/jcm.22.6.996-1006.1985

33. Wang X, Wang L, Wang Y, Tan R, Ke X, Zhou X, Geng J, Hou H, Zhou M (2017) Calcium sulfate hemihydrate whiskers obtained from flue gas desulfurization gypsum and used for the adsorption removal of lead. Crystals 7. https://doi.org/10.3390/cryst7090270
34. Şenol ZM, Elma E, El Messaoudi N, Mehmeti V (2023) Performance of cross-linked chitosan-zeolite composite adsorbent for removal of Pb2+ ions from aqueous solutions: experimental and Monte Carlo simulations studies. J Mol Liq 391. https://doi.org/10.1016/j.molliq.2023.123310
35. Elsayed NH, Monier M, Alatawi RAS, Al-Anazi M, Albalawi M, Alatawi MJ (2023) Selective removal of uranyl ions using ion-imprinted amino-phenolic functionalized chitosan. Int J Biol Macromol 237. https://doi.org/10.1016/j.ijbiomac.2023.124073
36. Elgarahy AM, Elwakeel KZ, Mohammad SH, Elshoubaky GA (2021) A critical review of biosorption of dyes, heavy metals and metalloids from wastewater as an efficient and green process. Clean Eng Technol 4:100209. https://doi.org/10.1016/j.clet.2021.100209
37. Şen NE, Şenol ZM (2023) Effective removal of Allura red food dye from water using cross-linked chitosan-diatomite composite beads. Int J Biol Macromol 253. https://doi.org/10.1016/j.ijbiomac.2023.126632
38. Langmuir I (1918) The adsorption of gases on plane surfaces of glass, mica and platinum. J Am Chem Soc 40. https://doi.org/10.1021/ja02242a004
39. Freundlich H (1907) Über die Adsorption in Lösungen. Zeitschrift Für Phys Chemie 57U. https://doi.org/10.1515/zpch-1907-5723
40. Rand B (1976) On the empirical nature of the Dubinin-Radushkevich equation of adsorption. J Colloid Interface Sci 56. https://doi.org/10.1016/0021-9797(76)90259-9
41. Hou L, Xing B, Guo H, Zeng H, Cheng S, Meng M, Qu X, Valdivieso López A, Zhang C, Cao Y (2023) Effect of mineralogical characteristics evolution of vermiculite upon thermal and chemical expansions on its adsorption behavior for aqueous Pb(II) removal. Powder Technol 430. https://doi.org/10.1016/j.powtec.2023.119040
42. Wang Q, Wang B, Lee X, Lehmann J, Gao B (2018) Sorption and desorption of Pb(II) to biochar as affected by oxidation and pH. Sci Total Environ 634. https://doi.org/10.1016/j.scitotenv.2018.03.189
43. Patel PK, Pandey LM, Uppaluri RVS (2023) Adsorptive removal of Zn, Fe, and Pb from Zn dominant simulated industrial wastewater solution using polyvinyl alcohol grafted chitosan variant resins. Chem Eng J 459. https://doi.org/10.1016/j.cej.2023.141563
44. Xu W, Liu X, Tang K (2022) Adsorption of hydroquinone and Pb(II) from water by β-cyclodextrin/polyethyleneimine bi-functional polymer. Carbohydr Polym 294. https://doi.org/10.1016/j.carbpol.2022.119806
45. Wang J, Zhang W (2021) Evaluating the adsorption of Shanghai silty clay to Cd(II), Pb(II), As(V), and Cr(VI): kinetic, equilibrium, and thermodynamic studies. Environ Monit Assess 193. https://doi.org/10.1007/s10661-021-08904-7
46. Lai KC, Lee LY, Hiew BYZ, Thangalazhy-Gopakumar S, Gan S (2020) Facile synthesis of xanthan biopolymer integrated 3D hierarchical graphene oxide/titanium dioxide composite for adsorptive lead removal in wastewater. Bioresour Technol 309. https://doi.org/10.1016/j.biortech.2020.123296
47. Şenol ZM, Şimşek S (2022) Insights into effective adsorption of lead ions from aqueous solutions by using chitosan-bentonite composite beads. J Polym Environ 30. https://doi.org/10.1007/s10924-022-02464-8
48. Ho YS, McKay G (1998) Kinetic models for the sorption of dye from aqueous solution by wood. Process Saf Environ Prot 76. https://doi.org/10.1205/095758298529326
49. Ho YS, McKay G (1999) Pseudo-second order model for sorption processes. Process Biochem 34. https://doi.org/10.1016/S0032-9592(98)00112-5
50. Weber WJ, Morris JC (1963) Kinetics of adsorption on carbon from solution. J Sanit Eng Div 89. https://doi.org/10.1061/jsedai.0000430
51. Elsayed NH, Monier M, Alatawi RAS, Al-Anazi M (2023) Design of ion-imprinted cellulose-based microspheres for selective recovery of uranyl ions. Carbohydr Polym 313. https://doi.org/10.1016/j.carbpol.2023.120873
52. Aljohani MS, Alnoman RB, Alharbi HY, Bukhari AAH, Monier M (2024) Development and evaluation of thiosalicylic-modified/ion-imprinted chitosan for selective removal of cerium (III) ion. Carbohydr Polym 326:121620. https://doi.org/10.1016/j.carbpol.2023.121620
53. Lima EC, Hosseini-Bandegharaei A, Moreno-Piraján JC, Anastopoulos I (2019) A critical review of the estimation of the thermodynamic parameters on adsorption equilibria. Wrong use of equilibrium constant in the Van't Hoof equation for calculation of thermodynamic parameters of adsorption. J Mol Liq 273. https://doi.org/10.1016/j.molliq.2018.10.048
54. Ebelegi AN, Ayawei N, Wankasi D (2020) Interpretation of adsorption thermodynamics and kinetics. Open J Phys Chem 10. https://doi.org/10.4236/ojpc.2020.103010
55. Borandegi M, Nezamzadeh-Ejhieh A (2015) Enhanced removal efficiency of clinoptilolite nano-particles toward Co(II) from aqueous solution by modification with glutamic acid. Colloids Surf A Physicochem Eng Asp 479. https://doi.org/10.1016/j.colsurfa.2015.03.040
56. Amin F, Talpur FN, Balouch A, Afridi HI (2017) Eco-efficient fungal biomass for the removal of Pb(II) ions from water system: a sorption process and mechanism. Int J Environ Res 11. https://doi.org/10.1007/s41742-017-0029-z
57. Yang S, Wang Y, Liu Y (2021) Biosorption of Cu(II) from aqueous solutions by a macrofungus (ganoderma lobatum) biomass and its biochar. Nat Environ Pollut Technol 20. https://doi.org/10.46488/NEPT.2021.v20i02.014
58. Isik B, Ugraskan V, Cankurtaran O (2022) Effective biosorption of methylene blue dye from aqueous solution using wild macrofungus (Lactarius piperatus). Sep Sci Technol 57. https://doi.org/10.1080/01496395.2021.1956540
59. Janeš D, Kreft S, Jurc M, Seme K, Štrukelj B (2007) Antibacterial activity in higher fungi (mushrooms) and endophytic fungi from Slovenia. Pharm Biol 45. https://doi.org/10.1080/13880200701575189
60. Szczepanski S, Lipski A (2013) Essential oils show specific inhibiting effects on bacterial biofilm formation. Food Control 36. https://doi.org/10.1016/j.foodcont.2013.08.023
61. Kapoor A, Viraraghavan T (1995) Fungal biosorption - an alternative treatment option for heavy metal bearing wastewaters: a review. Bioresour Technol 53. https://doi.org/10.1016/0960-8524(95)00072-M
62. Dhankhar R, Hooda A (2011) Fungal biosorption-an alternative to meet the challenges of heavy metal pollution in aqueous solutions. Environ Technol 32. https://doi.org/10.1080/09593330.2011.572922
63. Aragaw TA, Bogale FM (2021) Biomass-based adsorbents for removal of dyes from wastewater: a review. Front Environ Sci 9. https://doi.org/10.3389/fenvs.2021.764958
64. Michalak I, Chojnacka K, Witek-Krowiak A (2013) State of the art for the biosorption process - a review. Appl Biochem Biotechnol 170. https://doi.org/10.1007/s12010-013-0269-0